An investigation of correlation between left coronary bifurcation angle and hemodynamic changes in coronary stenosis by coronary computed tomography angiography-derived computational fluid dynamics

Zhonghua Sun[1], Thanapong Chaichana[2]

[1]Department of Medical Radiation Sciences, Curtin University, Perth, Australia; [2]Department of Mathematics and Computer Science, Liverpool Hope University, Liverpool, England, UK

Correspondence to: Professor Zhonghua Sun. Department of Medical Radiation Sciences, Curtin University, GPO Box, U1987, Perth, Western Australia 6845, Australia. Email: z.sun@curtin.edu.au.

Background: To investigate the correlation between left coronary bifurcation angle and coronary stenosis as assessed by coronary computed tomography angiography (CCTA)-generated computational fluid dynamics (CFD) analysis when compared to the CCTA analysis of coronary lumen stenosis and plaque lesion length with invasive coronary angiography (ICA) as the reference method.

Methods: Thirty patients (22 males, mean age: 59±6.9 years) with calcified plaques at the left coronary artery were included in the study with all patients undergoing CCTA and ICA examinations. CFD simulation was performed to analyze hemodynamic changes to the left coronary artery models in terms of wall shear stress, wall pressure and flow velocity, with findings correlated to the coronary stenosis and degree of bifurcation angle. Calcified plaque length was measured in the left coronary artery with diagnostic value compared to that from coronary lumen and bifurcation angle assessments.

Results: Of 26 significant stenosis at left anterior descending (LAD) and 13 at left circumflex (LCx) on CCTA, only 14 and 5 of them were confirmed to be >50% stenosis at LAD and LCx respectively on ICA, resulting in sensitivity, specificity, positive predictive value (PPV) and negative predictive value (NPV) of 100%, 52%, 49% and 100%. The mean plaque length was measured 5.3±3.6 and 4.4±1.9 mm at LAD and LCx, respectively, with diagnostic sensitivity, specificity, PPV and NPV being 92.8%, 46.7%, 61.9% and 87.5% for extensively calcified plaques. The mean bifurcation angle was measured 83.9±13.6° and 83.8±13.3° on CCTA and ICA, respectively, with no significant difference (P=0.98). The corresponding sensitivity, specificity, PPV and NPV were 100%, 78.6%, 84.2% and 100% based on bifurcation angle measurement on CCTA, 100%, 73.3%, 78.9% and 100% based on bifurcation angle measurements on ICA, respectively. Wall shear stress was noted to increase in the LAD and LCx models with significant stenosis and wider angulation (>80°), but demonstrated little or no change in most of the coronary models with no significant stenosis and narrower angulation (<80°).

Conclusions: This study further clarifies the relationship between left coronary bifurcation angle and significant stenosis, with angulation measurement serving as a more accurate approach than coronary lumen assessment or plaque lesion length for determining significant coronary stenosis. Left coronary bifurcation angle is suggested to be incorporated into coronary artery disease (CAD) assessment when diagnosing significant CAD.

Keywords: Angulation; coronary artery disease (CAD); calcification; coronary plaques; computational fluid dynamics (CFD); correlation; coronary computed tomography angiography (CCTA)

Introduction

Coronary computed tomography angiography (CCTA) is a widely used less-invasive imaging modality for the diagnosis of coronary artery disease (CAD) with high diagnostic accuracy achieved due to improved spatial and temporal resolution (1-5). Despite rapid developments of CT scanners and advanced imaging techniques, assessment of severely calcified coronary plaques is still challenging. Overestimation of the lumen stenosis resulting in high false positive rates is commonly seen in the presence of severe calcification in the coronary arteries due to blooming and beam-hardening artifacts which enlarge plaque volume and affect accurate visualization of the coronary lumen (6-8). This compromises the diagnostic value of CCTA, resulting in low specificity which is reported to range from 18% to 53% in patients with extensively calcified plaques (9-12).

Some strategies have been developed to improve visualization and assessment of calcified plaques, such as use of implementation of image processing algorithms or subtraction methods (13-15). However, the diagnostic accuracy of CCTA is still moderate in the presence of severe calcification in the coronary arteries. Another approach to overcome this limitation is to measure the left coronary bifurcation angle and determine the significance of CAD. Diagnostic value of CCTA with use of left bifurcation angle has been shown in a number of studies with improved diagnostic performance reported when compared to the coronary lumen assessment (16-21).

The reason of using bifurcation angle as another diagnostic approach is due to the fact that atherosclerosis tends to occur in the vascular tree with curved or bifurcation regions where wall shear stress is low or decreased, thus inducing atherosclerotic changes (22-25). Previous studies have showed the direct correlation between wide angulation and significant coronary stenosis or high-risk plaques (16,21,25). Investigation of hemodynamic changes due to different left coronary angulation has been performed to confirm the association between wide angulation and degree of coronary stenosis with use of CCTA-generated computational fluid dynamics (CFD) (25,26). However, there is a lack of detailed analysis of hemodynamic changes in relation to the characterization of calcified plaques such as focally or extensively calcified types, and plaque legion length. Thus, the purpose of this study is to further extend previous application of CCTA-derived CFD in the diagnostic assessment of calcified plaques with the aim of determining the clinical value of left coronary bifurcation

angle for diagnosis of significant coronary stenosis. In addition to assessments of coronary lumen stenosis and left bifurcation angle, we included another two parameters in this study, namely, the type of calcified coronary plaque in terms of focal or extensive calcification in relation to the extent of CAD, and plaque length with corresponding diagnostic value of determining significant stenosis. We hypothesized that the criterion of using left bifurcation angle for diagnosing significant coronary stenosis still holds true when compared to other approaches involving plaque morphological feature or coronary lumen analysis.

Methods

Participants

A retrospective review of patients who were referred for undergoing CCTA for diagnosis of CAD was conducted to identify CCTA images with only showing calcified coronary plaques at the left coronary artery with stenosis confirmed by invasive coronary angiography (ICA). Thirty patients (22 males, mean age: 59±6.9 years) were selected for this study as they had both CCTA and ICA examinations with calcified plaques detected at one or more left coronary arterial branches.

All patients were scanned with ≥64-detector row CT with details of scanning protocols described in previous studies (9,27). These latest CT scanners allow for acquisition of high-resolution images with isotropic voxel sizes between 0.4×0.4×0.4 and 0.6×0.6×0.6 mm^3, which is essential for generation of high quality patient-specific coronary 3D models for performing hemodynamic analysis.

Ethical approval was waived in this study due to the retrospective nature since CCTA and ICA examinations were part of routine diagnostic procedure for these patients. All of the images were de-identified with patient's details removed. Thus, informed consent was not required from the patients.

Measurement of coronary stenosis and left bifurcation angle

Degree of coronary stenosis was determining by measuring the minimal lumen diameter of the two main left coronary arteries, namely left anterior descending (LAD) and left circumflex (LCx). Measurements were performed on multiplanar reformatted images with the views showing the highest degree of stenosis due to calcified plaques. This has been described in our previous study (9).
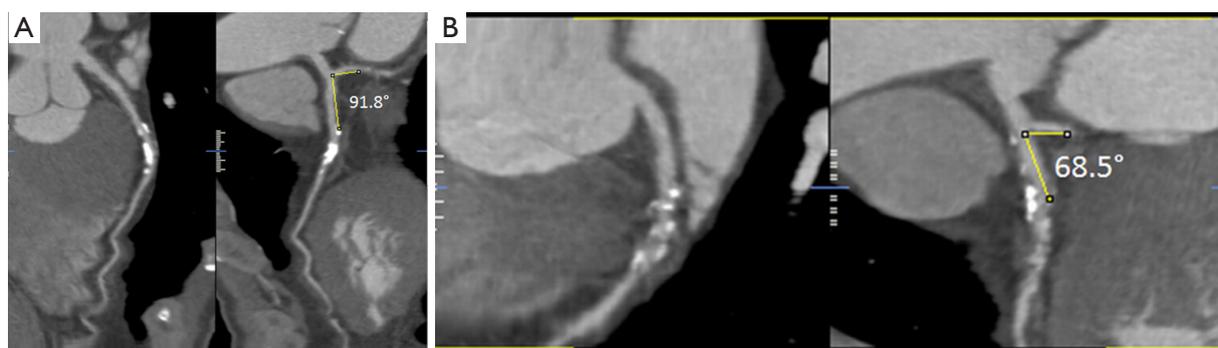
Figure 1 Curved planar reformatted images showing measurement of left bifurcation angle between left anterior descending and left circumflex, with wide and narrow angles measured in two different cases (A and B).
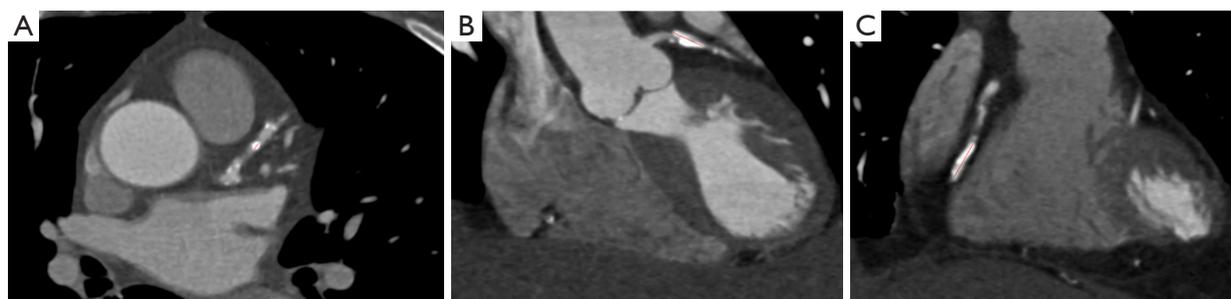
Figure 2 Coronary calcium length measurements to determine focally and extensively calcified plaques. (A) 2D axial image shows focal calcification in the left anterior descending (LAD) coronary artery with calcium length 2.89 mm; (B,C) coronary reformatted images show extensive calcifications at the LAD and left circumflex with calcium length measured 9.9 and 12.3 mm, respectively.

Left coronary artery branches form different bifurcation angles, including bifurcation angles between left main stem and LAD/LCx, and bifurcation angle between LAD and LCx. The bifurcation angle between LAD and LCx was used in this study as this is most commonly used to assess the CAD (*Figure 1*) (9,16-19). Measurements were performed on CCTA and ICA images by a radiologist with more than 10 years of experience in cardiac CT imaging.

Calcification of coronary plaques in the left coronary arteries was analyzed in terms of focal or extensive calcification based on measurement of the plaque length. The whole calcium length of more than 3.0 mm is considered to affect diagnostic accuracy of coronary CT angiography according to a recent study (28). Thus, the cut-off value of whole plaque length of 3.0 mm was implemented in this study to determine whether the calcified plaques belong to focal or extensive types as shown in *Figure 2*. Plaque length was measured in all patients with presence of calcified plaques at either LAD or LCx with the aim of determining diagnostic value of detecting significant coronary stenosis when compared to the reference method ICA.

Image postprocessing for generation of left coronary artery model

CCTA images were segmented using automatic and semi-automatic approaches to remove unwanted structured while keeping only the left coronary artery tree for flow dynamic analysis. Image processing and analysis of 3D volume datasets of CCTA were performed using Analyze 12.0 (Analyze Direct, Inc., Lexana, KS, USA) with details having been described in previous studies (25,26,28). In brief, the 3D objects were created to segment coronary artery tree from the cardiac CT volume data through the 'Object Separator' function that is available with Analyze 12.0. *Figure 3A-D* shows the step of image segmentation to extract coronary artery tree from the volume data, while *Figure 3E* is the 3D left coronary artery surface model which was saved in binary STL (stereolithography) format for generation of computational models.
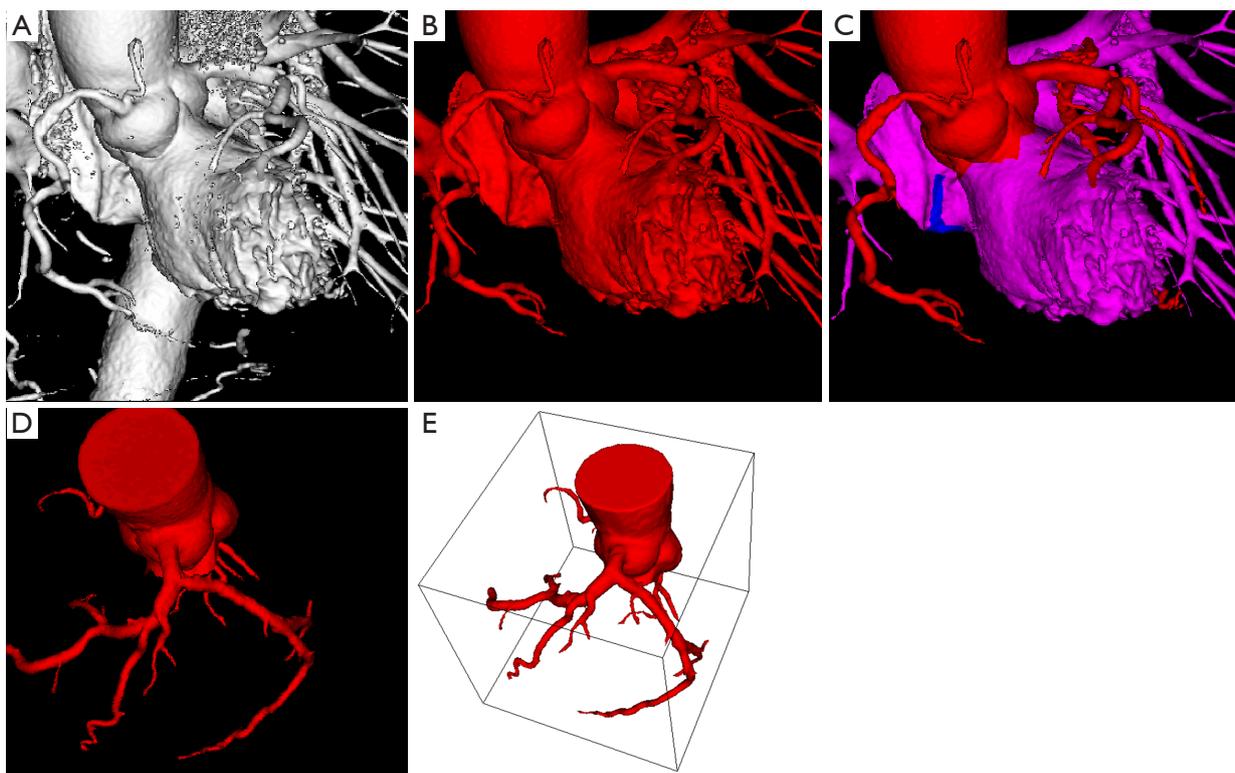
Figure 3 Segmentation steps showing the use of automatic and semi-automatic methods to extract coronary artery tree. (A) 3D volume rendering shows coronary arteries, ascending aorta, descending aorta and left ventricle; (B) part of aortic structures has been removed after applying automatic segmentation; (C) further image processing is performed to segment left ventricle and other structures (highlighted in pink color) while keeping the coronary artery tree; (D) coronary tree is segmented from other structures for modelling; (E) 3D coronary object model is viewed in stereolithography format.

The binary STL files were then imported into ANSYS ICEM CFD version 12 (ANSYS, Inc., Canonsburg, PA, USA), and the hexahedral meshes were configured to range approximately 3×10^5 to 1×10^6 for all computations with steps having been described in previous studies (25,29). The meshes were transferred to ANSYS CFX version 12 (ANSYS, Inc.) using the CFX5 format for CFD computations.

CFD simulation for hemodynamic analysis

The actual simulation of *in vivo* conditions of blood flow in the left coronary artery was considered using realistic human physiological information for initial conditions of three-dimensional numerical computations. The time dependent computations were performed for calculations of hemodynamic changes using accurate hemodynamic rheology and material properties, as used in previous studies (25,26). Pulsatile physiological conditions were configured as inlet and outlets of left coronary bifurcation artery branches, and 1,060 kg/m^3 of blood density and 0.0035 Pa·s of blood viscosity was also configured for appropriate rheological parameters (25,26). Blood flow was modeled as laminar flow with no-slip condition at arterial walls with assumed rigid wall model. Incompressible fluid and Newtonian blood were configured for the blood flow simulation. Navier Stokes equations were used to govern calculation of flow hemodynamics by ANSYS CFX version 12 on a 32-bit Microsoft Windows 7, 6 GB RAM, Xeon W3505 CPU 2.53 GHz. The CFD calculations were run at 0.0125 seconds per time step for 80-time steps representing one cardiac cycle. The residual targets were setup at less than 1×10^{-4} for each computation and the calculated simulations were converged using total time around 3–8 hours, depending upon the size of meshing element models. Post-processing computational results were done

in ANSYS CFD-Post version 12 (ANSYS, Inc.), and wall shear stress, flow velocity and wall pressure were calculated and analyzed for computational assessment of left coronary bifurcation angle with hemodynamic changes.

Statistical analysis

Data were entered into SPSS software for statistical analysis (SPSS 24.0, IBM Corporation, Armonk, NY, USA). Continuous variables were expressed as mean ± standard deviation, while categorical variables were presented as percentages. Chi-square test was used for analysis of categorical variables. One sample *t*-test was used to determine the differences in left coronary bifurcation angle measured between CCTA and ICA. Diagnostic value in terms of sensitivity, specificity, positive predictive value (PPV) and negative predictive value (NPV) was calculated and compared based on coronary lumen assessment and plaque length measured on CCTA, and bifurcation angle measured on CCTA and ICA with ICA as the reference standard to determine significant stenosis. A P value of <0.05 was considered statistically significant.

Results

Patient characteristics with inclusion of plaque type and location in the left coronary arteries with corresponding degree of lumen stenosis and left bifurcation angle are shown in *Table 1*. The mean left bifurcation angle between LAD and LCx was measured 83.9±13.6°, and 83.8±13.3°, on CCTA and ICA images, respectively with no significant difference (P=0.98).

Calcified plaques were found in at least one of the left coronary arteries, with significant stenosis detected in 26 LAD and 13 LCx on CCTA images. However, only 14 (53%) and 5 (38%) of them were confirmed to be >50% stenosis on ICA, resulting in diagnostic sensitivity, specificity, PPV and NPV of CCTA of 100%, 52%, 49% and 100%. When the cut-off value of >3.0 mm was used to determine extensive calcification/or significant stenosis, 21 (72%) and 7 (35%) of them were extensively calcified plaques at LAD and LCx, respectively. The mean calcified plaque length was measured 5.3±3.6 and 4.4±1.9 mm at LAD and LCx. The sensitivity, specificity, PPV and NPV were 92.8%, 46.7%, 61.9% and 87.5% for extensively calcified plaques, showing slight improvements in PPV but decreased specificity when compared to those from lumen assessment.

Although the bifurcation angle measured on extensively calcified plaques was larger than that measured on focally calcified plaques, there was no significant difference between these two types of calcified plaques on both CCTA and ICA measurements (88.4±13.3° and 89.0±13.7° for extensively calcified plaques on CCTA and ICA; 81.2±13.4° and 81.3±12.6° for focally calcified plaques on CCTA and ICA) (P=0.13 to 0.16). With use of >80° as a cut-off value to determine significant stenosis, diagnostic specificity and PPV were 78.6% and 84.2% based on bifurcation angle measured on CCTA, 73.3% and 78.9% based on bifurcation angle measured on ICA, respectively, while the sensitivity and NPV of 100% remained the same for these two approaches.

Table 1 also shows the hemodynamic changes related to the coronary plaques and bifurcation angles. In comparison with coronary lumen assessment, WSS was found to have a direct correlation with bifurcation angle, with wider angulation (>80°) and significant stenosis showing increased WSS, while in contrast, in the coronary models with narrower angulation, WSS remained no significant changes in most of the cases. Wall pressure was noted to decrease in coronary stenosis with wide angulation and flow velocity was increased at post-stenotic lesions at the LAD and LCx with significant stenosis. *Figures 4* and *5* are examples showing CFD analysis of hemodynamic changes in patients with narrow and wide angulations.

Discussion

This study extends our previous report to further analyze the hemodynamic changes in relation to the type of calcified plaque, lumen stenosis and bifurcation angle. There are three findings arising from this study which are considered to contribute to the current literature: first, coronary lumen stenosis is not reliable in assessing calcified plaques due to high false positive rates resulting in low specificity and PPV. Second, left coronary bifurcation angle is associated with significant coronary stenosis with subsequent hemodynamic changes, in particular, the WSS changes in these stenotic lesions, showing more accurate assessment of calcified coronary lesions. Third, although detailed plaque characterization of calcification in the coronary arteries enables determination of significant coronary stenosis with extensively calcified plaques showing improved PPV, the diagnostic value is still low in detecting calcified plaques, further confirming the limited accuracy with use of plaque morphology assessment.

542

Sun and Chaichana. CCTA-derived CFD in coronary plaques

Table 1 Correlation of CFD simulations with coronary CT angiography and invasive angiography findings

| No. of cases	Bifurcation angle (°)		Type of calcification (E/F)	Degree of lumen stenosis on CCTA		Degree of lumen stenosis on ICA		CFD analysis			Risk assessment
	CCTA	ICA		LAD	LCx	LAD	LCx	WSS	Wall pressure	Flow velocity	Angulation/lumen
1	99	99.5	F	74%	33%	89%	25%	High at LAD stenotic site	Decreased at LAD stenotic site	Increased at LAD stenotic site	◄
2	78	70	F	62%	–	44%	–	No significant change	Slightly decreased at LAD	Slightly turbulent at LAD	✓
3	53	55.7	F	80%	65%	42%	48%	No significant change	No significant change	Laminar flow	✓
4	105	105	F	72%	87%	44%	77%	Increased at LAD and LCx	Decreased at LCx stenotic site	High at LCx stenotic site	►
5	68.5	75	E	72%	–	25%	–	No significant change	No significant change	Laminar flow	✓
6	91.8	90	F	69%	–	29%	–	No significant change	No significant change	Laminar flow	✓
7	108	115	E	60%	26%	15%	2%	Increased at LAD	No significant change	High at LAD	►
8	76.2	77	F	88%	68%	28%	45%	Slightly increased at LM	No significant change	Slight increased at LM and LAD	►
9	91.5	85	F	61%	49%	61%	5%	High at LAD stenotic site	No significant change	Slight increased at LAD	◄
10	74	78	F	57%	71%	39%	48%	No significant change	No significant change	Laminar flow	✓
11	71.3	70.7	E	51%	–	19%	–	High at LM	No significant change	Slightly increased at LM	►
12	75.7	73.5	F	–	74%	–	36%	High at LCx	No significant change	Increased at LCx	✓
13	109	112	E	75%	–	70%	–	Decrease at LAD stenotic site	No significant change	Decreased at LAD stenotic site	◄
14	84.9	85	F	68%	–	–	18%	High at LAD stenotic site	No significant change	Increased at LAD stenotic site	◄
15	80.3	80	F	44%	66%	24%	79%	High at LAD stenotic site	No significant change	Decreased at LAD and LCx	◄
16	84	80.6	F	56%	–	81%	–	High at LM and LAD stenotic site	Decreased at LAD stenotic site	Increased at LM and LAD stenotic site	◄
17	61	75.5	F	44%	47%	20%	15%	High at LM and LAD stenotic site	Decreased at LAD stenotic site	Increased at LM and LAD stenotic site	►
18	77	78	F	83%	–	32%	–	Decreased at LAD stenotic site	No significant change	Decreased at LAD and Increased at LCx	✓

Table 1 (*continued*)

qims.amegroups.com *Quant Imaging Med Surg* 2017;7(5):537-548

Table 1 (*continued*)

No. of cases	Bifurcation angle (°)		Type of calcification (E/F)	Degree of lumen stenosis on CCTA		Degree of lumen stenosis on ICA		CFD analysis			Risk assessment
	CCTA	ICA		LAD	LCx	LAD	LCx	WSS	Wall pressure	Flow velocity	Angulation/lumen
19	82	81	E	80%	26%	64%	18%	Increased at LAD stenotic site	Decreased at LAD stenotic site	Laminar flow	√
20	81	81	E	81%	63%	76%	51%	Decreased at LAD	No significant change	Slightly turbulent at LAD	√
21	82	86.5	E	59%	60%	75%	45%	Decreased at LCx	No significant change	Decreased at LCx	√
22	89	86.3	F	70%	58%	91%	87%	High at LM and LAD stenotic site	No significant change	Increased at LM and LAD stenotic site	√
23	98	91	E	70%	47%	72%	13%	No significant change	No significant change	High at LM	√
24	89	85	E	79%	72%	66%	44%	High at LAD stenotic site	Decreased at LAD stenotic site	Increased at LAD stenotic site	▼
25	100	99.5	F	73%	–	63%	–	High at LAD stenotic site	Decreased at LAD stenotic site	Increased at LAD stenotic site	▲
26	86.3	83	F	67%	–	61%	–	Increased at LAD	Decreased at LAD stenotic site	High at LAD	▲
27	96	91	E	82%	–	58%	–	High at LAD stenotic site	Decreased at LAD stenotic site	Increased at LAD stenotic site	▲
28	88.3	91	E	69%	76%	58%	59%	High at LCx stenotic site	Decreased at LAD and LCx stenotic sites	Increased at LAD and LCx stenotic sites	▼
29	65.8	59	F	65%	63%	20%	42%	Increased at LAD	Slightly decreased at LAD	High at LAD	√
30	71	75	F	47%	57%	45%	32%	High at LAD stenotic site	No significant change	Increased at LAD stenotic site	√

▲, high risk of coronary stenosis and angulation; ▼, low risk of coronary stenosis and angulation; √, normal coronary lumen with no risk of developing significant stenosis. CCTA, coronary CT angiography; ICA, invasive coronary angiography; LM, left main stem; LAD, left anterior descending; LCx, left circumflex; WSS, wall shear stress; F, focally calcified coronary plaques; E, extensively calcified plaques.

544

Sun and Chaichana. CCTA-derived CFD in coronary plaques
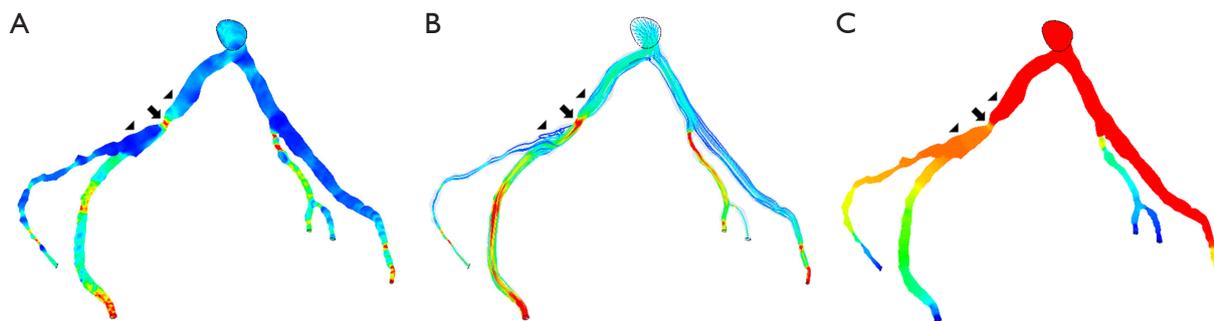
Figure 4 Correlation between wider angulation and hemodynamic changes by CCTA-derived computational fluid dynamic (CFD) analysis. Left coronary bifurcation angle was measured 105° between the two main arterial branches, left anterior descending (LAD) and left circumflex (LCx) with significant stenosis (>70%) at LCx on CCTA and ICA in a 58-year-old man. CFD analysis shows increased wall shear stress and flow velocity at the stenotic site of LCx (A,B), while decreased wall pressure at the same location (C). Arrow refers to the stenotic region at LCx, while arrowheads point to the pre- and post-stenotic locations. Reprint with permission under the open access from (26).
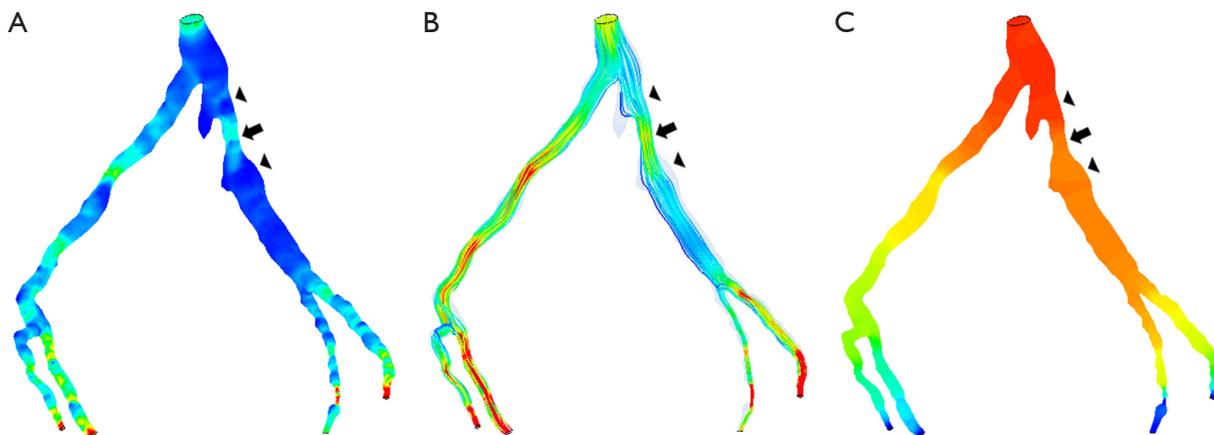
Figure 5 Correlation between narrower angulation and CCTA-derived computational fluid dynamic (CFD) analysis. Left coronary bifurcation angle was measured 53° and 55.7° between LAD and LCx on CCTA and ICA in a 65-year-old male, respectively. Significant stenosis (>60%) was noticed at LAD and LCx on CCTA, but no significant stenosis (42–48%) was confirmed on ICA (images not shown). No significant change was observed with wall shear stress, flow velocity and wall pressure (A-C). Arrow refers to the mild stenotic site of LAD, while arrowheads point to the pre- and post-stenotic locations. Reprint with permission under the open access from (26).

Use of 50% stenosis as a cut-off value to determine coronary stenosis is known to be unreliable in predicting functional significance. This has led to the increasing use of CCTA-derived hemodynamic analysis in the diagnosis of CAD, with CCTA-derived fractional flow reserve (FFR_{CT}) as a hot topic in the current literature (30-32). Multicenter studies have showed the superiority of FFR_{CT} over CCTA for diagnosis of ischemic coronary lesions with overall improved diagnostic accuracy (33-36). The recently published FFR_{CT} RIPCORD study has shown that the routine use of FFR_{CT} has changed patient management

when compared to CCTA alone (36). FFR_{CT} was calculated in 200 patients with stable chest pain undergoing CCTA for clinical diagnosis. With FFR_{CT} incorporated into diagnostic approach, there was a change in patient management in 36% cases. The discrepancy between FFR_{CT} and CCTA is due to discordance in the assessment of lesion severity, with FFR_{CT} found >0.8 in nearly 30% cases which were determined as significant stenosis of >90% by CCTA. This further emphasizes the enhanced value of using hemodynamic analysis for assessment of coronary lesions.

Use of left coronary bifurcation angle as another

criterion in diagnosing CAD has been increasingly reported in the literature with improved diagnostic accuracy when compared to conventional CCTA (16-21). A cut-off value of 80° is recommended by these studies to decide the significance of coronary stenosis. This is also confirmed in this study with wider angulations (>80°) associated with hemodynamic changes when compared to narrower angulations. This is in accordance with previous reports based on realistic and patient-specific coronary models showing the direct correlation between coronary angulation and corresponding hemodynamic changes (25,26,37-40). In their recent study, Park *et al.* analyzed hemodynamic features in relation to different types of coronary plaques based on CCTA-generated CFD models in 80 patients with plaques distributed at the left coronary artery (40). Their results showed that WSS offers additional information than coronary lumen stenosis in determining plaque features, in particular, differentiating high-risk plaques from stable ones. Findings of this study are consistent with their results showing that WSS changes in coronary arteries in wide angulation are associated with significant coronary stenosis, indicating hemodynamic significance. This study focuses on analysis of calcified coronary plaques because this is a challenging area for CCTA due to high false positive rates resulting from blooming artifacts. Thus, results add valuable information to the existing literature.

Although CCTA is an excellent imaging modality in the detection and diagnosis of CAD, its diagnostic value is hindered by presence of severe calcification in the coronary arteries, which leads to low specificity and PPV (9-12). Despite use of different strategies to suppress the effect of heavy calcification on coronary lumen stenosis (13-15), heavily calcified plaques still present a major challenge in CCTA. This is also confirmed in this study with specificity and PPV around 50% (49–52%) based on analysis of calcified plaque in the left coronary arteries. However, when analyzing plaque distribution in the coronary arteries, the PPV of CCTA in extensively calcified plaque was slightly improved from 52% to 61.9%, but with decreased other values when compared to that from coronary lumen assessment. The low diagnostic value of CCTA (<70% for specificity and PPV) based on plaque morphology is in agreement with a recent study (30). Tesche *et al.* compared morphological parameters of coronary plaques with functional significance of coronary plaques for determining lesion-specific ischemia with invasive FFR as the reference standard (30). No significant correlation was found between calcified plaque volume/lesion length and hemodynamically significant coronary stenosis, highlighting that plaque feature analysis, especially for calcified plaques is not a reliable parameter (30,41). Use of bifurcation angle to assess coronary stenosis has further improved the specificity and PPV to nearly 80% as shown in our studies through a head-to-head comparison between CCTA and ICA (9,27). Results of this study further justify the use of bifurcation angle to predict significant coronary stenosis due to its association with hemodynamic changes.

There are some limitations in this study that should be acknowledged. First, the sample size is relatively small, in particular, the number of cases with significant stenosis confirmed in ICA is small. In addition, we only focused on calcified plaques in this study, while excluding other types of plaques. Thus, results of this study need to be interpreted with caution with regard to the improved diagnostic value of CCTA using bifurcation angle measurements. Further studies with inclusion of more cases with inclusion of all types of plaques are desirable. Second, CCTA-derived CFD modeling was based on coronary artery models with rigid wall. Fluid-structure interaction with consideration of coronary wall change during cardiac cycles is considered to provide insights into elucidating the relationship between calcified plaques with different angles and coronary hemodynamics. Finally, as discussed previously, FFR_{CT} represents a new direction in identifying lesion-specific ischemia, and this was not performed in this study due to the lack of correlation with invasive FFR which is the gold standard. More robust conclusion could be drawn with FFR_{CT} added to the analysis of calcified plaques in relation to bifurcation angles.

In conclusion, this study further advances previous research on the improved diagnostic value of using left coronary bifurcation angle for more accurate assessment of coronary stenosis. Calcified coronary plaques with wider angulation are associated with significant stenosis as represented by hemodynamic changes, mainly with increased wall shear stress and flow velocity. Coronary lumen stenosis on CCTA is associated with low specificity and PPV. Although characterization of calcified plaques shows slight improvements in PPV with extensively calcified plaques based on plaque length analysis, the corresponding diagnostic specificity and positive predictive value still remain low. Further research on a large cohort with incorporation of CCTA-derived CFD analysis into characterization of plaque types and left bifurcation angle is warranted.

546

Sun and Chaichana. CCTA-derived CFD in coronary plaques

Acknowledgements

Footnote

Conflicts of Interest: The authors have no conflicts of interest to declare.

Ethical Statement: Ethical approval was waived in this study due to the retrospective nature since CCTA and ICA examinations were part of routine diagnostic procedure for these patients. All of the images were de-identified with patient's details removed. Thus, informed consent was not required from the patients.

References

1. Sun Z, Choo GH, Ng KH. Coronary CT angiography: current status and continuing challenges. Br J Radiol 2012;85:495-510.

2. Saremi F, Achenbach S. Coronary plaque characterization using CT. AJR Am J Roentgenol 2015;204:W249-60.

3. Xu L, Yang L, Fan Z, Yu W, Lv B, Zhang Z. Diagnostic performance of 320-detector CT coronary angiography in patients atrial fibrillation. Eur Radiol 2011;21:936-43.

4. Flohr TG, De Cecco CN, Schmidt B, Wang R, Schoepf UJ, Meinel FG. Computed tomographic assessment of coronary artery disease: state-of-the-art imaging techniques. Radiol Clin N Am 2015;53:271-85.

5. Sun Z, Al Moudi M, Cao Y. CT angiography in the diagnosis of cardiovascular disease: a transformation in cardiovascular CT practice. Quant Imaging Med Surg 2014;4:376-96.

6. Zhang LJ, Wu SY, Wang J, Lu Y, Zhang ZL, Jiang SS, Zhou CS, Lu GM. Diagnostic accuracy of dual-source CT coronary angiography: the effect of average heart rate, heart rate variability, and calcium score in a clinical perspective. Acta Radiol 2010;51:727-40.

7. Gang S, Min L, Li L, Guo-Ying L, Lin X, Qun J, Hua Z. Evaluation of CT coronary artery angiography with 320-row detector CT in a high-risk population. Br J Radiol 2012;85:562-70.

8. Uehara M, Funabashi N, Takaoka H, Fujimoto Y, Kobayashi Y. False-positive findings in 320-slice cardiac CT for detection of severe coronary stenosis in comparison with invasive coronary angiography indicate poor prognosis for occurrence of MACE. Int J Cardiol

2014;172:235-7.

9. Sun Z, Xu L, Fan Z. Coronary CT angiography in calcified coronary plaques: comparison of diagnostic accuracy between bifurcation angle measurement and coronary lumen stenosis for diagnosing significant coronary stenosis. Int J Cardiol 2016;203:78-86.

10. Park MJ, Jung JI, Choi YS, Ann SH, Youn HJ, Jeon GN, Choi HC. Coronary CT angiography in patients with high calcium score: evaluation of plaque characteristics and diagnostic accuracy. Int J Cardiovasc Imaging 2011;27:43-51.

11. Chen CC, Chen CC, Hsieh IC, Liu YC, Liu CY, Chan T, Wen MS, Wan YL. The effect of calcium score on the diagnostic accuracy of coronary computed tomography angiography. Int J Cardiovasc Imaging 2011;Suppl 1:37-42.

12. Palumbo AA, Maffei E, Martini C, Tarantini G, Di Tanna GL, Berti E, Grilli R, Casolo G, Brambilla V, Cerrato M, Rotondo A, Weustink AC, Mollet NR, Cademartiri F. Coronary calcium score as gatekeeper for 64-slice computed tomography coronary angiography in patients with chest pain: per-segment and per-patient analysis. Eur Radiol 2009;19:2127-35.

13. Sun Z, Ng CK, Xu L, Fan Z, Lei J. Coronary CT angiography in heavily calcified coronary arteries: improvement of coronary lumen visualization and coronary stenosis assessment with image processing methods. Medicine 2015;94:e2148.

14. Takx RAP, Willemink MJ, Nathoe HM, Schilham AM, Budde RP, de Jong PA, Leiner T. The effect of iterative reconstruction on quantitative computed tomography assessment of coronary plaque composition. Int J Cardiovasc Imaging 2014;30:155-63.

15. Tanaka R, Yoshioka K, Muranaka K, Chiba T, Ueda T, Sasaki T, Fusazaki T, Ehara S. Improved evaluation of calcified segments on coronary CT angiography: a feasibility study of coronary calcium subtraction. Int J Cardiovasc Imaging 2013;29:75-81.

16. Sun Z, Cao Y. Multislice CT angiography assessment of left coronary artery: Correlation between bifurcation angle and dimensions and development of coronary artery disease. Eur J Radiol 2011;79:e90-5.

17. Kawasaki T, Koga H, Serikawa T, Orita Y, Ikeda S, Mito T, Gotou Y, Shintani Y, Tanaka A, Tanaka H, Fukuyama T, Koga N. The bifurcation study using 64 multislice computed tomography. Catheter Cardiovasc Interv 2009;73:653-58.

18. Pflederer T, Ludwig J, Ropers D, Daniel WG, Achenbach S. Measurement of coronary artery bifurcation angles

by multidetector computed tomography. Invest Radiol 2006;41:793-8.

19. Cui Y, Zeng W, Yu J, Lu J, Hu Y, Diao N, Liang B, Han P, Shi H. Quantification of left coronary bifurcation angles and plaques by coronary computed tomography angiography for prediction of significant coronary stenosis: A preliminary study with dual-source CT. PloS One 2017;12:e0174352.

20. Juan YH, Tsay PK, Shen WC, Yeh CS, Wen MS, Wan YL. Comparison of the Left Main Coronary Bifurcating Angle among Patients with Normal, Non-significantly and Significantly Stenosed Left Coronary Arteries. Sci Rep 2017;7:1515.

21. Temov K, Sun Z. Coronary computed tomography angiography investigation of the association between left main coronary artery bifurcation angle and risk factors of coronary artery disease. Int J Cardiovasc Imaging 2016;32:129-37.

22. Rodriguez-Granillo GA, Garcia-Garcia HM, Wentzel J, Valgimigli M, Tsuchida K, van der Giessen W, de Jaegere P, Regar E, de Feyter PJ, Serruys PW. Plaque composition and its relationship with acknowledged shear stress patterns in coronary arteries. J Am Coll Cardiol 2006;47:884-5.

23. Markl M, Wegent F, Zech T Bauer S, Strecker C, Schumacher M, Weiller C, Hennig J, Harloff A. In vivo wall shear stress distribution in the carotid artery: Effect of bifurcation geometry, internal carotid artery stenosis, and recanalization therapy. Circ Cardiovasc Imaging 2010;3:647-55.

24. Arjmandi Tash O, Razavi SE. Numerical investigation of pulsatile blood flow in a bifurcation model with a non-planar branch: The effect of different bifurcation angles and nonplanar branch. Bioimpacts 2012;2:195-205.

25. Chaichana T, Sun Z, Jewkes J. Computation of hemodynamics in the left coronary artery with variable angulations. J Biomech 2011;44:1869-78.

26. Sun Z, Chaichana T. Computational fluid dynamic analysis of calcified coronary plaques: correlation between hemodynamic changes and cardiac image analysis based on left coronary bifurcation angle and lumen assessments. Interv Cardiol 2016;8:713-9.

27. Xu L, Sun Z. Coronary CT angiography evaluation of calcified coronary plaques by measurement of left coronary bifurcation angle. Int J Cardiol 2015;182:229-31.

28. Kruk M, Noll D, Achenbach S, Mintz GS, Pręgowski J, Kaczmarska E, Kryczka K, Pracoń R, Dzielińska Z, Sleszycka J, Witkowski A, Demkow M, Rużyłło W, Kępka

C. Impact of coronary artery calcium characteristics on accuracy of CT angiography. JACC Cardiovasc Imaging 2014;7:49-58.

29. Chaichana T, Sun Z, Jewkes, J. Computational fluid dynamics analysis of the effect of plaques in the left coronary artery. Comput Math Methods Med 2012;2012:504367.

30. Tesche C, De Cecco CN, Caruso D, Baumann S, Renker M, Mangold S, Dyer KT, Varga-Szemes A, Baquet M, Jochheim D, Ebersberger U, Bayer RR 2nd, Hoffmann E, Steinberg DH, Schoepf UJ. Coronary CT angiography derived morphological and functional quantitative plaque markers correlated with invasive fractional flow reserve for detecting hemodynamically significant stenosis. J Cardiovasc Comput Tomogr 2016;10:199-206.

31. Cheruvu C, Naoum C, Blanke P, Norgaard B, Leipsic J. Beyond stenosis with fractional flow reserve via computed tomography and advanced plaque analysis for the diagnosis of lesion –specific ischemia. Can J Cardiol 2016;32:1315. e1-1315.e9.

32. Ko BS, Cameron JD, Munnur RK, Wong DTL, Fujisawa Y, Sakaguchi T, Hirohata K, Hislop-Jambrich J, Fujimoto S, Takamura K, Crossett M, Leung M, Kuganesan A, Malaiapan Y, Nasis A, Troupis J, Meredith IT, Seneviratne SK. Noninvasive CT-derived FFR based on structural and fluid analysis: A comparison with invasive FFR for detection of functionally significant stenosis. JACC Cardiovasc Imaging 2017;10:663-73.

33. Koo BK, Erglis A, Doh JH, Daniels DV, Jegere S, Kim HS, Dunning A, DeFrance T, Lansky A, Leipsic J, Min JK. Diagnosis of ischemia-causing coronary stenoses by noninvasive fractional flow reserve computed from coronary computed tomographic angiograms. Results from the prospective multicenter discover-flow (diagnosis of ischemia-causing stenoses obtained via noninvasive fractional flow reserve) study. J Am Coll Cardiol 2011;58:1989-97.

34. Min JK, Berman DS, Budoff MJ, Jaffer FA, Leipsic J, Leon MB, Mancini GB, Mauri L, Schwartz RS, Shaw LJ. Rationale and design of the DeFACTO (Determination of Fractional Flow Reserve by Anatomic Computed Tomographic AngiOgraphy) study. J Cardiovasc Comput Tomogr 2011;5:301-9.

35. Nørgaard BL, Leipsic J, Gaur S, Seneviratne S, Ko BS, Ito H, Jensen JM, Mauri L, De Bruyne B, Bezerra H, Osawa K, Marwan M, Naber C, Erglis A, Park SJ, Christiansen EH, Kaltoft A, Lassen JF, Bøtker HE, Achenbach S; NXT Trial Study Group. Diagnostic performance of non-

548

Sun and Chaichana. CCTA-derived CFD in coronary plaques

invasive fractional flow reserve derived from coronary CT angiography in suspected coronary artery disease: The NXT trial. J Am Coll Cardiol 2014;63:1145-55.

36. Curzen NP, Nolan J, Zaman AG, Norgaard BL, Rajani R. Does the routine availability of CT-derived FFR influence management of patients with stable chest pain compared to CT angiography alone? The FFRCT RIPCORD Study. JACC Cardiovasc Imaging 2016;9:1188-94.

37. Chaichana T, Sun Z, Jewkes J. Hemodynamic impacts of various types of stenosis in the left coronary artery bifurcation: A patient-specific analysis. Phys Med 2013;29:447-52.

38. Dong J, Sun Z, Inthavong K, Tu J. Fluid-structure interaction analysis of the left coronary artery with variable branch angulation. Comput Methods Biomech Biomed Engin 2015;18:1500-8.

39. Beier S, Ormiston J, Webster M, Cater J, Norris S,

Medrano-Gracia P, Young A, Cowan B. Impact of bifurcation angle and other anatomical characteristics on blood flow-A computational study of non-stented and stented coronary arteries. J Biomech 2016;49:1570-82.

40. Park JB, Choi G, Chun EJ, Kim HJ, Park J, Jung JH, Lee MH, Otake H, Doh JH, Nam CW, Shin ES, De Bruyne B, Taylor CA, Koo BK. Computational fluid dynamic measures of wall shear stress are related to coronary lesion characteristics. Heart 2016;102:1655-61.

41. Diaz-Zamudio M, Dey D, Schuhbaeck A, Nakazato R, Gransar H, Slomka PJ, Narula J, Berman DS, Achenbach S, Min JK, Doh JH, Koo BK. Automated quantitative plaque burden from coronary CT angiography noninvasively predicts hemodynamic significance by using fractional flow reserve in intermediate coronary lesions. Radiology 2015;276:408-15.